

Sensitivity of an underwater Čerenkov km³ telescope to TeV neutrinos from Galactic Microquasars

S. Aiello^c, M. Ambriola^a, F. Ameli^k, I. Amore^{e,d},
 M. Anghinolfi^g, A. Anzalone^e, G. Barbarino^h, E. Barbarito^a,
 M. Battaglieri^g, R. Bellotti^a, N. Beverini^j, M. Bonori^k,
 B. Bouhadef^j, M. Brescia^{h,i}, G. Cacopardo^e, F. Cafagna^a,
 A. Capone^k, L. Caponetto^c, E. Castorina^j, A. Ceres^a,
 T. Chiarusi^k, M. Circella^a, R. Cocimano^e, R. Coniglione^e,
 M. Cordelli^f, M. Costa^e, S. Cuneo^g, A. D'Amico^e,
 G. De Bonis^k, C. De Marzo^{a,1}, G. De Rosa^h, R. De Vita^g,
 C. Distefano^{e,*}, E. Falchini^j, C. Fiorello^a, V. Flaminio^j,
 K. Fratini^g, A. Gabrielli^b, S. Galeotti^j, E. Gandolfi^b,
 G. Giacomelli^b, F. Giorgi^b, A. Grimaldi^c, R. Habel^f,
 E. Leonora^{c,d}, A. Lonardo^k, G. Longo^h, D. Lo Presti^{c,d},
 F. Lucarelli^k, E. Maccioni^j, A. Margiotta^b, A. Martini^f,
 R. Masullo^k, R. Megna^a, E. Migneco^{e,d}, M. Mongelli^a,
 T. Montaruli^{l,2}, M. Morganti^j, M. Musumeci^e, C.A. Nicolau^k,
 A. Orlando^e, M. Osipenko^g, G. Osteria^h, R. Papaleo^e,
 V. Pappalardo^e, C. Petta^{c,d}, P. Piattelli^e, G. Raia^e,
 N. Randazzo^c, S. Reito^c, G. Ricco^g, G. Riccobene^e,
 M. Ripani^g, A. Rovelli^e, M. Ruppi^a, G.V. Russo^{c,d}, S. Russo^h,
 P. Sapienza^e, M. Sedita^e, E. Shirokov^g, F. Simeone^k,
 V. Sipala^{c,d}, M. Spurio^b, M. Taiuti^g, G. Terreni^j, L. Trasatti^f,
 S. Urso^c, V. Valente^f, P. Vicini^k,

^aINFN Sezione Bari and Dipartimento Interateneo di Fisica Università di Bari,
Via E. Orabona 4, 70126, Bari, Italy

^bINFN Sezione Bologna and Dipartimento di Fisica Università di Bologna, V.le
Berti Pichat 6-2, 40127, Bologna, Italy

^cINFN Sezione Catania, Via S.Sofia 64, 95123, Catania, Italy

^dDipartimento di Fisica and Astronomia Università di Catania, Via S.Sofia 64,
95123, Catania, Italy

^e*INFN Laboratori Nazionali del Sud, Via S.Sofia 62, 95123, Catania, Italy*

^f*INFN Laboratori Nazionali di Frascati, Via Enrico Fermi 40, 00044, Frascati (RM), Italy*

^g*INFN Sezione Genova and Dipartimento di Fisica Università di Genova, Via Dodecaneso 33, 16146, Genova, Italy*

^h*INFN Sezione Napoli and Dipartimento di Scienze Fisiche Università di Napoli, Via Cintia, 80126, Napoli, Italy*

ⁱ*INAF Osservatorio Astronomico di Capodimonte, Salita Moiarriello 16, 80131, Napoli, Italy*

^j*INFN Sezione Pisa and Dipartimento di Fisica Università di Pisa, Polo Fibonacci, Largo Bruno Pontecorvo 3, 56127, Pisa, Italy*

^k*INFN Sezione Roma 1 and Dipartimento di Fisica Università di Roma "La Sapienza", P.le A. Moro 2, 00185, Roma, Italy*

^l*University of Wisconsin, Department of Physics, 53711, Madison, WI, USA*

Abstract

In this paper are presented the results of Monte Carlo simulations on the capability of the proposed NEMO-km³ telescope to detect TeV muon neutrinos from Galactic microquasars. For each known microquasar we compute the number of detectable events, together with the atmospheric neutrino and muon background events. We also discuss the detector sensitivity to neutrino fluxes expected from known microquasars, optimizing the event selection also to reject the background; the number of events surviving the event selection are given.

Key words: Microquasars, Neutrino telescopes, NEMO

PACS: 95.55.Vj, 95.85.Ry, 96.40.Tv

1 Introduction

The realization of a km³ scale detector for astrophysical high energy neutrinos is one of the most important scientific goals of astroparticle physics. Due to their small interaction cross section, high energy neutrinos are expected to

* Fax: +39 095 542 398

Email address: distefano_c@lns.infn.it (C. Distefano).

¹ Deceased

² On leave of absence Dipartimento Interateneo di Fisica Università di Bari, Via E. Orabona 4, 70126, Bari, Italy

allow us to observe into dense environments in our Universe and to extend our knowledge beyond the distances that can be explored with γ -rays and cosmic ray observatories [1,2].

A number of astrophysical sources of high energy neutrinos, both galactic (SuperNova remnants, microquasars, ...) and extragalactic (Active Galactic Nuclei, Gamma Ray Bursts, ...), have been proposed. Since neutrino production requires a hadronic component inside the jet, neutrino detection will be a fundamental probe to investigate jet composition and particle acceleration processes taking place in these sources.

The main aim of this paper is to study the sensitivity of the proposed NEMO-km³ telescope [3] to high energy neutrinos emitted by known microquasars. In particular we simulated the interaction of microquasar muon-neutrinos inside and in the proximity of the NEMO-km³ neutrino telescope in order to estimate the expected muon event rate. In our calculations we accounted for the atmospheric neutrino and muon fluxes reaching the detector in order to optimize the event selection and reconstruction procedures.

2 Neutrino fluxes from microquasars

Microquasars are Galactic X-ray binary systems which exhibit relativistic jets, observed in the radio band. The presence of an accretion disc and relativistic jets make microquasars similar to *small* quasars (see ref. [4]). Several authors propose microquasar jets as sites of acceleration of charged particles up to energies of about 10^{16} eV, and of high energy neutrino production.

Levinson & Waxman [5] proposed a theoretical model for neutrino emission from microquasar jets, considering the production of neutrinos from the interactions of protons, accelerated in the jet, with synchrotron photons, emitted by electrons, or with external X-ray photons of the accretion disk. According to this model, microquasars may be intense sources of high energy muon neutrinos, in the energy range between 1 and 100 TeV. Applying the Levinson & Waxman model, Distefano et al. [6] estimated the expected neutrino fluxes from an ensemble of known microquasars, showing that several of these sources may be identified with the future km³ neutrino telescopes.

Bednarek [7] considers the case of microquasars in which a Wolf-Rayet star supplies matter onto the compact object. Together with the scenario proposed by Levinson and Waxman, Bednarek considers also two regions where high energy neutrinos may be produced. In the jet region II (see ref.[7]) neutrons resulting from photo-disintegration of accelerated nuclei produce neutrinos after interactions with the inner disk matter. In the jet region III the process takes

place in the proximity of the Wolf-Rayet star surface. In particular Bednarek discusses the case of Cygnus X-3 and calculates the neutrino spectra (see Fig. 2 in [7]) produced by a power-law spectrum of nuclei $\gamma_A^{-\kappa}$, exploring different possible values for the spectral index κ and for the Lorentz factor cut-off γ_A^{max} . Another component of the neutrino flux may arise from neutrons injected by mono-energetic nuclei having a Lorentz factor $\gamma_A^{min} \approx 10^5$.

Aharonian et al. [8] discuss different possible scenarios for the production of the γ -ray flux recently observed from LS 5039 by the HESS Collaboration [9]. They consider both leptonic and hadronic production mechanisms and argue in favor of a TeV photon flux originating from pp interactions. They suggest therefore that the γ -ray flux should be accompanied by a TeV neutrino flux of about $10^{-12} \text{ cm}^{-2} \text{ s}^{-1}$, or even a factor of 100 larger.

In this paper we discuss the results obtained simulating neutrino fluxes calculated with the three models reported above.

Christiansen et al. [10] recently published predictions on the emission of high energy neutrinos from “windy microquasars”. Their calculations, based on the model proposed by Romero et al. [11], describe the emission of high energy neutrinos and γ -rays from pions created in the inelastic collision between relativistic protons ejected by the compact object and ions in the stellar wind. As an example they consider microquasar LS I +61 303, estimating an average event rate of 3-5 TeV muon neutrinos per kilometer-square per year. This source is outside the field of view of a Mediterranean neutrino telescope, but their model can be applied to other possible sources such as LS 5039, Cygnus X-3, and Cygnus X-1, which are observable from the Northern Hemisphere.

Romero & Orellana [12] discuss the case of microquasars that show strongly misaligned jets with respect to the perpendicular to the orbital plane. If the donor star is an early-type star, the jet could collide with the stellar wind, producing γ -rays and neutrinos. The expected neutrino fluxes are in general too low to be detected by the planned km^3 telescopes and are not considered in this paper.

3 The NEMO project

The NEMO Collaboration [13] is performing R&D towards the design and construction of the Mediterranean km^3 neutrino detector. The activity was mainly focused on the search and characterization of an optimal site for the detector installation and on the development of a feasibility study for the detector.

After eight years of activities in seeking and monitoring marine sites in the central Mediterranean Sea, the Collaboration selected a large marine area (centered at the coordinates Lat. $36^{\circ} 25'$ N, Long. $16^{\circ} 00'$ E) located about 80 km from the Southern cape of Sicily, Capo Passero, in the Ionian Sea plateau as optimal site for the deployment of the km^3 telescope. The measured average values of the absorption length for blue light (440 nm) is ~ 70 m, close to the one of optically pure sea salt water; measurements also show that seasonal variations of the light absorption length are negligible [14]. The optical background, measured at ~ 3000 m depth and for a 10" PMT at 0.5 s.p.e. threshold, has an average rate of 30 kHz, compatible with the noise expected from ^{40}K decay. An exhaustive report on the Capo Passero site properties is available in [14,15].

NEMO proposes a preliminary project for the km^3 detector based on present technological and budget constraints. The detector architecture consists of a square array of structures called towers, hosting the optical modules and the instrumentation. The tower is a three dimensional flexible structure composed of a sequence of "storeys" (which host the instrumentation) interlinked by a system of cables and anchored on the seabed. The structure is kept vertical by an appropriate buoyancy on the top. In its working position each storey will be rotated by 90° , with respect to the upper and lower adjacent ones, around the vertical axis of the tower. The final features of the tower (number and length of storeys, number of optical modules per storey, distance between the storeys, distance between the towers) is under study with the goal of optimizing the detector performance.

The km^3 telescope, simulated in this paper, is a square array of 9×9 towers with a distance between towers of 140 m. In this configuration each tower hosts 72 PMTs (with a diameter of 10"), namely 5832 PMTs for the whole detector with a total geometrical volume of $\sim 0.9 \text{ km}^3$. We considered an 18 storey tower; each storey is made of a 20 m long beam structure hosting two optical modules (one downlooking and one looking horizontally) at each end (4 OMs per storey). The vertical distance between storeys is 40 m. A spacing of 150 m is added at the base of the tower, between the anchor and the lowermost storey.

As an intermediate step to ensure an adequate process of validation, NEMO is building a demonstrator which includes most of the critical elements of the proposed km^3 detector: NEMO Phase-1 [13]. It is under realization at the Underwater Test Site of the Laboratori Nazionali del Sud in Catania, where a 28 km electro optical cable, reaching the depth of 2000 m, allows the connection of deep sea instrumentation to a shore station. The NEMO Phase-1 system will be composed of a junction box and a mini-tower (with 4 storeys). This should allow to test the proposed mechanical solutions as well as the data transmission, the power distribution, the timing calibration and the acoustic

positioning systems. NEMO Phase-1 should be operating at the end of 2006.

Although the Phase-1 project will provide a fundamental test of the technologies proposed for the realization and installation of the detector, these must be finally validated at the depths needed for the km³ detector. For these motivations the realization of an infrastructure on the site of Capo Passero has been undertaken [13].

A further R&D program will also be developed by the Collaboration within the KM3NeT Design Study [16].

4 The simulation codes

In this section we describe the simulation tools and procedures to study the detector response to high energy neutrinos. As a first step we generated samples of muon events having vertexes within an appropriate volume of water. Three sets of muon samples were generated: atmospheric muons, muons induced by atmospheric neutrinos and muons induced by neutrinos coming from point-like astrophysical sources. These events were then propagated inside the detector, using the simulation tools developed by the ANTARES Collaboration [17] described in ref. [18]. The codes simulate the emission and the propagation of Čerenkov light radiated by muons and their secondary products, then record photo-electrons signals on PMTs. Subsequently, background signals due to the ⁴⁰K decay are generated in an appropriate time window and added to the event. Another code [18] is then used to reconstruct muon tracks. These codes, developed for detector configurations with smaller size and different geometries, were modified for a larger geometry, as described in [19,20]. A brief description of the simulation steps is given in the following.

4.1 Generation of neutrino-induced muon events at the detector

Neutrino-induced muon events are generated using the event generation code developed by the ANTARES Collaboration [18]. The code generates neutrinos that interact inside and in the proximity of the detector, producing detectable muons. Interacting neutrinos are generated with a power law spectrum ε_{ν}^{-X} , where X is a generic spectral index. These events are weighted, as described below, in order to reproduce the expected spectrum. The direction of incident neutrinos coming from a point-like source is generated taking into account the change of the relative position of the astrophysical sources with respect to the detector rest frame, due to the Earth rotation. In the case of a diffuse neutrino flux, such as atmospheric neutrinos, the neutrino direction is generated with

an isotropic distribution.

Once the interacting neutrino is generated (i.e. neutrino energy ε_ν , direction $(\vartheta_\nu, \varphi_\nu)$, interaction vertex (x, y, z) and event weight W_{event} are assigned), the code simulates the neutrino Charged Current weak interaction, producing the muon kinematics. Since the detection efficiency of the detector is poor for muon energies lower than 100 GeV [20], the lowest neutrino energy considered in the simulations is 100 GeV. At these energies, the main contribution to the neutrino interaction, is from Deep Inelastic Scattering (DIS), here simulated using the code LEPTO [21]. Once the neutrino-induced muons are generated, they are propagated up to the surface of the detector sensitive volume. This volume is defined as a cylinder with size large enough that the Čerenkov light emitted outside its volume has a negligible probability to reach any PMT. In particular, the cylinder size extends beyond the instrumented volume by 3 times the blue light absorption length (~ 70 m). The muon propagation is performed using the code MUSIC [22].

In the generation procedure a weight W_{event} is assigned to each event in order to normalize the number of generated events to the expected neutrino flux. The event weight is calculated multiplying the expected neutrino spectrum $(dn_\nu/d\varepsilon_\nu dS dt)^{expected}$ (evaluated at the generated neutrino energy and direction) times the generation weight W_{gen} :

$$W_{event} = W_{gen} \cdot \left(\frac{dn_\nu}{d\varepsilon_\nu dS dt} \right)^{expected}. \quad (1)$$

W_{gen} is defined as the inverse of the simulated neutrino spectrum. In the case of a diffuse neutrino flux, it is given by:

$$W_{gen}^{-1} = \frac{\varepsilon_\nu^{-X}}{I_E I_\vartheta} \cdot \frac{N_{total}}{t_{gen}} \cdot \frac{1}{V_{gen}} \cdot \frac{1}{\sigma_{CC}(\varepsilon_\nu) \rho N_A} \cdot \frac{1}{P_{Earth}(\varepsilon_\nu, \vartheta_\nu)}, \quad (2)$$

where X is the generation spectral index, I_E is the integral of the generation spectrum shape ε_ν^{-X} over the whole simulated neutrino energy range, I_ϑ is the integral of the solid angle in which events are generated. N_{total} is the number of simulated events and t_{gen} is the event generation time. The neutrino interaction vertices are randomly generated within the volume V_{gen} that completely contains the detector sensitive volume and with size large enough that neutrinos interacting outside cannot produce detectable muons. In particular, its size extends beyond the detector sensitive volume by the maximum range covered by the neutrino-induced muons. $(\sigma_{CC}(\varepsilon_\nu) \rho N_A)^{-1}$ is the neutrino CC interaction length in a medium of density ρ , $\sigma_{CC}(\varepsilon_\nu)$ is the CC neutrino interaction cross section and N_A is the Avogadro number. Eq.(2) takes also into account the neutrino absorption in the Earth, through the transmission prob-

ability $P_{Earth}(\varepsilon_\nu, \vartheta_\nu)$, which depends on neutrino energy and direction [23]. In the case of a point-like source neutrinos, the factor I_ϑ does not appear in relation 2.

4.2 Generation of atmospheric muons

Atmospheric muons are generated according to the Okada formula [24], which parameterizes the integral energy spectrum of muons, reaching a given depth D in seawater, as a function of the muon energy and direction. Since this parameterization is a complicated function of many parameters, a weighted generation procedure, similar to the one used for neutrino events, is used. Muon energies are generated with a given spectral index X and muon directions are isotropically generated, in 2π solid angle (only downward directed). For each generated event a weight W_{event} is calculated multiplying the Okada atmospheric muon spectrum times the generation weight W_{gen}

$$W_{gen} = \frac{\varepsilon_\mu^X I_E I_\vartheta t_{gen} A_{geom}}{N_{total}}, \quad (3)$$

where A_{geom} is the detection geometrical area, i.e. the detector sensitive surface, projected on a plane perpendicular to the incident muon direction. The other parameters have the same meaning as in Eq.(2). In order to take into account the detector height ($\simeq 1$ km), the Okada spectrum is evaluated at the depth where the muon track intersects the detector sensitive volume.

4.3 Muon propagation inside the detector

The subsequent simulation steps of the simulation are: the propagation of muons inside the detector, the generation of the Čerenkov photons and the simulation of the PMT response. The muon propagation is performed with MUSIC [22] in order to take into account high energy radiative processes like bremsstrahlung. The Čerenkov light produced by secondary electrons is also taken into account. In the code we take into account the light absorption length as a function of wavelength, according to the water optical properties measured in the Capo Passero site. Once the PMT hits are generated, spurious PMT hits, due to the underwater optical noise (^{40}K decays), are introduced. It is assumed that optical background produces uncorrelated single photoelectron (s.p.e.) signals in the PMTs. The PMT response function is taken into account. In the simulations made for this work the optical background signals are generated assuming an average rate of 30 kHz for 10" PMTs, corresponding to the average value measured in Capo Passero.

4.4 Event reconstruction

It is possible to reconstruct the direction of the muon track, using information from arrival times of photons in the PMTs, hit amplitudes (proportional to the number of photo-electrons in the PMTs) and PMT positions. The used reconstruction strategy aims at the rejection of hits due to background and selects a sub-set of hits compatible with the muon track. The track reconstruction algorithm used in this work is a robust track fitting procedure based on a maximum likelihood method [25].

In order to reduce the number of hits due to background the first step consists in the rejection of hits with amplitude smaller than 0.5 p.e. then a causality filter with respect to the highest amplitude hit is applied³. The causality filter used in this work is based on the following condition:

$$(|dt| - dr/v < 20 \text{ ns}) \text{ AND } (|dt| - dr/c < 500 \text{ ns}), \quad (4)$$

where $|dt|$ is the absolute value of the time delay between two hits, dr is the distance between the PMTs where the hits are detected, v is the group velocity of light in water. The first condition is based on the fact that the front propagation of direct Čerenkov photons moves in water with velocity $v \approx c/n$ ($n = 1.35$). The second condition takes into account that, in the case of large distances, light absorption does not allow Čerenkov photons to propagate far from the initial muon track. The value of 500 ns takes into account the late Čerenkov photons, due to light scattering, δ -rays and showers.

The reconstruction algorithm starts with a linear prefit applied on a sub-set of hits that passed the causality criterion and in which there are at least three hits that satisfy the following trigger condition: the hit has an amplitude higher than 3.5 p.e. or the hit belongs to a “local coincidence”. A local coincidence is defined as two or more simultaneous hits ($\Delta t \leq 20$ ns) in the two PMTs at the bar edge. Starting from the result of the pre-fit, a sequence of fit procedures using all the hits that passed the causality criterion is applied. A further hit rejection based on the track parameters is also applied.

5 Results of simulations: events from point-like sources

In this section the results of the simulation of the passage of muons originated by neutrinos from microquasars in the NEMO-km³ telescope are presented.

³ This is an important step since the number of noise hits may be comparable or larger than the number of muon hits in case of high noise rate or low muon energy.

For each source, a number $N_{total} = 10^9$ of interacting neutrinos was simulated in the energy range 1 - 100 TeV in order to reproduce the neutrino fluxes calculated by Distefano et al. [6]. The generation spectral index is chosen to be $X = 1$, in order to guarantee a good event statistics at the highest energies. For microquasar LS 5039, $N_{total} = 10^8$ events were generated in the energy range 0.1 - 1 TeV to simulate neutrinos events according to the model proposed by Aharonian et al. [8]. For microquasar Cygnus X-3, $N_{total} = 10^8$ events were generated in the energy range 0.1 - 1 TeV and $N_{total} = 10^9$ events with energies 100 - 1000 TeV to simulate Bednarek's theoretical fluxes [7].

We present only results concerning microquasars observable, below the Astronomical Horizon, by a telescope located in the Capo Passero site (i.e. with declination $\delta \lesssim +54^\circ$).

5.1 Number of detectable events from microquasars

In Tab. 1 we give the theoretical neutrino fluxes calculated by Distefano et al. [6] and the number of muon events reconstructed using the simulation described above. Results refer to an integration time Δt equal to the duration of the considered burst for the transient sources and to one year for the steady sources.

In Tab. 2 the number of muon events from LS 5039 according to the model of Aharonian et al. [8] is given. The simulations refer to a power-law neutrino spectrum, $dn_\nu/d\varepsilon_\nu \propto \varepsilon_\nu^{-\Gamma}$, with energy cutoff $\varepsilon_\nu^{max} = 10$ TeV and 100 TeV, and $\Gamma = 1.5$ and 2, respectively. For the four combinations of parameters Γ and ε_ν^{max} , an average neutrino energy flux $f_\nu^{th} = 10^{-10}$ erg/cm² s ($\varepsilon_\nu > 0.1$ TeV) was simulated.

In Tab. 3 we give the number of muon events from Cygnus X-3 according to Bednarek [7] estimates considering different values of the parameters κ and γ_A^{max} and for mono-energetic nuclei.

5.2 "Neutrino image" of a point-like source

Using the information on reconstructed muon directions we computed the equatorial coordinates (declination and right ascension) of the detected muons, and we mapped the reconstructed events in equatorial coordinates. This allows to obtain an image of the source and to evaluate the spread of the reconstructed muon directions (due to neutrino interactions and to the muon track reconstruction error) around the source coordinates.

Table 1

Expected number of neutrino induced muons from the Levinson and Waxman microquasar model: N_{μ}^{exp} is the total number of reconstructed muons from each microquasar expected from the theoretical neutrino energy flux f_{ν}^{th} quoted by Distefano et al. [6], during the time interval Δt . We also report the expected number N_{μ}^m of selected muon neutrino events during the time Δt and the atmospheric background events N_{μ}^b surviving the event selection and expected in 1 year of data taking (see section 7).

Source name	Δt (days)	f_{ν}^{th} (erg/cm ² s)	N_{μ}^{exp}	N_{μ}^m	N_{μ}^b
<i>Steady Sources</i>					
LS 5039	365	$1.69 \cdot 10^{-12}$	0.2	0.1	0.1
Scorpius X-1	365	$6.48 \cdot 10^{-12}$	0.8	0.2	0.1
SS433	365	$1.72 \cdot 10^{-9}$	205.0	76.0	0.1
GX 339-4	365	$1.26 \cdot 10^{-9}$	185.0	68.0	0.1
Cygnus X-1	365	$1.88 \cdot 10^{-11}$	2.0	0.5	0.1
<i>Bursting Sources</i>					
XTE J1748-288	20	$3.07 \cdot 10^{-10}$	2.2	0.8	0.3
Cygnus X-3	3	$4.02 \cdot 10^{-9}$	3.4	0.8	0.1
GRO J1655-40	6	$7.37 \cdot 10^{-10}$	1.7	0.6	0.1
GRS 1915+105	6	$2.10 \cdot 10^{-10}$	0.4	0.1	< 0.1
Circinus X-1	4	$1.22 \cdot 10^{-10}$	0.2	0.1	0.1
XTE J1550-564	5	$2.00 \cdot 10^{-11}$	< 0.1	< 0.1	< 0.1
V4641 Sgr	0.3	$2.25 \cdot 10^{-10} \div 3.25 \cdot 10^{-8}$	< 0.1 \div 4.6	< 0.1 \div 1.4	0.1
GS 1354-64	2.8	$1.88 \cdot 10^{-11}$	< 0.1	< 0.1	0.1
GRO J0422+32	1 \div 20	$2.51 \cdot 10^{-10}$	0.1 \div 1.5	< 0.1 \div 0.4	0.1
XTE J1118+480	30 \div 150	$5.02 \cdot 10^{-10}$	2.4 \div 12.0	1.0 \div 4.8	0.2

The 2D angular distribution of the reconstructed muons for SS433 and GX339-4 (the two persistent microquasars expected to produce the largest number of events) is plotted in Fig. 1. It is important to note that the shape of the images depend on the source theoretical spectral indices ($\Gamma = 2$) and on the energy range for simulated microquasar neutrino fluxes.

Table 2

Expected number of neutrino induced muons from microquasar LS 5039 (Aharonian et al. model [8]): N_{μ}^{exp} is the total number of reconstructed muons from LS 5039 during an interval time of 1 year. We also give the number N_{μ}^m from the source compared to the atmospheric background events N_{μ}^b surviving the event selection (see section 7).

LS 5039				
Γ	ε_{ν}^{\max} (TeV)	N_{μ}^{exp}	N_{μ}^m	N_{μ}^b
1.5	10	7.0	1.7	0.2
1.5	100	15.0	4.9	0.1
2.0	10	4.3	1.0	0.3
2.0	100	9.0	2.6	0.1

Table 3

Expected number of neutrino induced events from microquasar Cygnus X-3 (Bednarek model [7]): N_{μ}^{exp} is the total number of reconstructed muons from Cygnus X-3 during an interval time of 1 year. We also report the number N_{μ}^m from the source compared to the atmospheric background muons N_{μ}^b surviving the event selection (see section 7).

Cygnus X-3	REG. II	REG. III	REG. II	REG. III	
κ, γ_A^{\max}	N_{μ}^{exp}	N_{μ}^{exp}	N_{μ}^m	N_{μ}^m	N_{μ}^b
2.0, 10^6	2.0	1.8	0.4	0.4	0.1
2.0, 10^7	5.2	5.0	1.1	1.1	0.1
2.5, 10^7	0.3	0.2	< 0.1	0.1	0.1
mono-energetic	< 0.1	4.5	< 0.1	0.7	0.1

6 Results of simulations: background events

6.1 Atmospheric neutrino background simulation

In order to evaluate the contribution of the atmospheric neutrino background with respect to the signal produced by a point-like neutrino source, we simulated a total number $N_{total} = 5.1 \cdot 10^{10}$ interacting atmospheric neutrinos, with a generation spectral index $X = 2$. Neutrinos were generated in the energy range 100 GeV - 10^8 GeV with a 4π isotropic angular distribution. The total number of reconstructed neutrino-induced muons is about $6.6 \cdot 10^5$. The atmospheric neutrino events are weighted to the sum of the Bartol flux [26] and of the `rqpm` model [27] to take into account the contribution of prompt

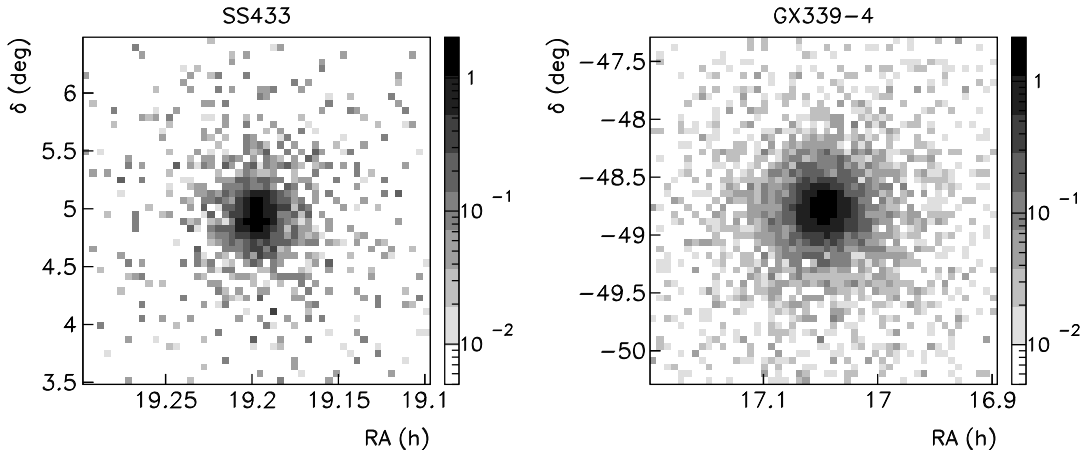


Fig. 1. Weighted event distributions for the microquasars SS433 and GX339-4, referring to 1 year of data taking. Both maps are obtained from 2D histograms with $0.06^\circ \times 0.06^\circ$ bin size.

neutrinos. Considering an observation time of 1 year, the total weighted number of reconstructed atmospheric neutrinos (up-going + down-going) is about $4.7 \cdot 10^4$.

6.2 Atmospheric muon background simulation

Atmospheric muon events are generated applying a weighted generation technique. We generated $N_{total} = 2.5 \cdot 10^7$ muons, in the energy range 1 TeV - 1 PeV, with a spectral index $X = 3$. We also generated $N_{total} = 4 \cdot 10^7$ events in the range 100 GeV - 1 TeV, with a spectral index $X = 1$. Muons are generated with an isotropic distribution as described in sec. 4.2; the number of reconstructed events is about $3.8 \cdot 10^6$. According to the Okada parameterization, the expected number of reconstructed muons is about $4 \cdot 10^8$ per year. The statistics of the generated muon sample is large enough to simulate only a few days of data taking. Since reconstructed events have a flat distribution in Right Ascension (RA), it is possible to project the full sample of simulated events in a few degrees bin ΔRA . This allows to get statistics of atmospheric muon background corresponding to a time of ~ 1 year of data taking for a region of a few degrees around each single source (the exact detector data taking time interval is a function of the bin-width ΔRA and of the declination).

At this level the fraction of background events is very high. In order to reduce it, an event selection is applied, as discussed in the next section.

7 NEMO-km³ sensitivity to microquasars neutrino fluxes

7.1 Criteria for atmospheric muon background rejection

The used reconstruction algorithm is a robust track fitting procedure based on a maximization likelihood method [25]. In this work, we used, as a *goodness of fit criterion*, the variable:

$$\Lambda \equiv -\frac{\log(\mathcal{L})}{N_{DOF}} + 0.1(N_{comp} - 1), \quad (5)$$

where $\log(\mathcal{L})/N_{DOF}$ is the log-likelihood per degree of freedom (N_{DOF}) and N_{comp} is the number of solutions found by the reconstruction program (see ref. [25] for details). This quality cut is applied together with the selection criteria listed here:

- the muon must be reconstructed with $\vartheta_{\mu}^{rec} < \vartheta_{\mu}^{max}$, in order to reject down-going events;
- the variable Λ must be greater than a given value Λ_{cut} ;
- only events reconstructed in a circular sky region centered in the source position and having a radius of r_{bin} are considered.

The optimal values of ϑ_{μ}^{max} , Λ_{cut} and r_{bin} are chosen to optimize the detector sensitivity as discussed in the next section.

7.2 Detector sensitivity to neutrino fluxes from microquasars

The detector sensitivity was calculated according to the Feldman and Cousins approach [28]. The 90% c.l. sensitivity to a neutrino flux coming from a point-like source is given by

$$f_{\nu,90} = \frac{\bar{\mu}_{90}(b)}{N_{\mu}} f_{\nu,0}, \quad (6)$$

where $\bar{\mu}_{90}(b)$ is the 90% c.l. average upper limit for an expected background with known mean value b and no true signal [28], $f_{\nu,0}$ is an arbitrary point source flux inducing a mean signal N_{μ} . The detector sensitivity was calculated for a livetime of 1 year, simulating a neutrino flux with spectral index $\Gamma = 2$ in the energy range 1 - 100 TeV and taking into account both atmospheric neutrino and muon background. The study was carried out for each microquasar, since the sensitivity is a function of the source astronomical declination. In

Tab. 4 we give the sensitivity for each microquasar, and the corresponding ϑ_{μ}^{max} , Λ_{cut} and r_{bin} . The dependence of the sensitivity on the source declination is shown in Fig. 2; the sensitivity flux limit increases with increasing declination, due to the decrease of the time per day spent by the source below the Astronomical Horizon (with respect to the latitude of the Capo Passero site).

In Tab. 5 are summarized the detector sensitivities for microquasar LS 5039, assuming neutrino fluxes with spectral indices $\Gamma = 1.5$ and 2, in the energy range 0.1 TeV and $\varepsilon_{\nu}^{max} = 10$ and 100 TeV.

We applied the event selection cuts given in Tab. 4 and 5 to determine the expected number of events from theoretical models considered in this paper. In Tab. 1 we give the number of selected neutrino events from each microquasar in a time interval Δt , according to the neutrino fluxes given by Distefano et al. [6]. In the same table we compare these results with the atmospheric neutrino and muon background in 1 year of data taking. In this analysis, it is assumed that transient sources cause one burst per year, i.e. the number of source events produced in the interval Δt is related to 1 year observation time.

In order to estimate the event rates for non-persistent sources it is crucial to know their duty cycle. Some of these sources have a periodic bursting activity: Circinus X-1 has a period of 16.59 days [29]. This means therefore that we expect about 1.5 events per year. Other transient sources show a stochastic bursting activity. For such cases it is difficult to give an estimate of the expected event rate. For example, during 1994 GRO J1655-40 showed three radio flares, each lasting 6 days [30]; during the same year GRS 1915+105 emitted 4 bursts [31]. A recent study [32] has shown that microquasars GRS 1915+105, Cygnus X-3 and Scorpius X-1 are in flaring mode the 21, 10 and 3 percent of the time, respectively. The possibility to integrate over more than one burst could therefore help to detect neutrinos from microquasars.

The search for neutrino events in coincidence with microquasar radio outbursts could be a tool to reject atmospheric background, restricting the analysis period to the flare duration Δt . Such an analysis technique, already used by AMANDA [33], can improve the detector sensitivity to neutrinos from transient sources. Referring to the bursts considered in Tab. 1 and integrating over the time interval Δt , we expect an average background of about 10^{-3} events (muons) per burst. Therefore, a cumulative analysis of all bursting microquasars could be possible. For instance, summing on the bursts in Tab. 1, we count $2.4 \div 4.9$ events from microquasars and only 0.04 background events.

For the microquasar LS 5039 we considered the flux predicted by Aharonian et al. [8]. The expected number of selected events is given in Tab. 2; the comparison with the atmospheric background shows that an evidence could be expected in a few years of data taking.

In Tab. 3 we quote the expected number of events from microquasar Cygnus X-3, according to the Bednarek model [7]. Since the model predicts a neutrino flux with a spectral index close to 2 and since the main event contribution is in the energy range 1 - 100 TeV, we used the same event selection parameters quoted in Tab. 4. In the case of $\kappa = 2.5$ and $\gamma_A^{max} = 10^7$ the signal is lower than the background. In the other cases, the number of events exceeds the expected background. The signal could be therefore detected in a few years of data taking, especially in the case of $\kappa = 2$ and $\gamma_A^{max} = 10^7$ with 2.2 events per year.

Table 4

Detector sensitivity to neutrinos from microquasars: the sensitivity f_ν is calculated for an ε_ν^{-2} neutrino spectrum in the energy range 1 - 100 TeV, for a detector live time of 1 year. The corresponding values of ϑ_μ^{max} , Λ_{cut} and r_{bin} and the source declination δ are also given.

Source name	ϑ_μ^{max} (deg)	Λ_{cut}	r_{bin} (deg)	f_ν (erg/cm ² s)	δ (deg)
<i>Steady Sources</i>					
LS 5039	101	-7.3	0.9	$6.5 \cdot 10^{-11}$	-14.85
Scorpius X-1	104	-7.7	0.7	$5.8 \cdot 10^{-11}$	-15.64
SS433	115	-8.0	0.8	$5.7 \cdot 10^{-11}$	4.98
GX 339-4	96	-7.4	0.5	$4.7 \cdot 10^{-11}$	-48.79
Cygnus X-1	103	-7.5	0.7	$9.0 \cdot 10^{-11}$	35.20
<i>Bursting Sources</i>					
XTE J1748-288	102	-7.6	0.9	$5.4 \cdot 10^{-11}$	-28.47
Cygnus X-3	101	-7.3	0.8	$1.1 \cdot 10^{-10}$	40.95
GRO J1655-40	101	-7.4	0.7	$5.2 \cdot 10^{-11}$	-39.85
GRS 1915+105	100	-7.4	0.8	$7.4 \cdot 10^{-11}$	10.86
Circinus X-1	90	-7.3	0.9	$4.2 \cdot 10^{-11}$	-56.99
XTE J1550-564	90	-7.1	0.9	$4.4 \cdot 10^{-11}$	-56.48
V4641 Sgr	102	-7.4	0.9	$5.6 \cdot 10^{-11}$	-25.43
GS 1354-64	90	-7.5	1.0	$3.8 \cdot 10^{-11}$	-64.73
GRO J0422+32	103	-7.5	0.8	$8.7 \cdot 10^{-11}$	32.91
XTE J1118+480	102	-7.5	0.7	$1.1 \cdot 10^{-10}$	48.05

Table 5

Detector sensitivity flux to neutrinos from LS 5039: the sensitivity f_ν is calculated for a $\varepsilon_\nu^{-\Gamma}$ neutrino spectrum in the energy range from 0.1 TeV up to ε_ν^{max} and for a detector live time of 1 year. The corresponding values of ϑ_μ^{max} , Λ_{cut} and r_{bin} are also given.

Γ	ε_ν^{max} (TeV)	ϑ_μ^{max} (deg)	Λ_{cut}	r_{bin} (deg)	f_ν (erg/cm ² s)
1.5	10	101	-7.3	1.0	$1.5 \cdot 10^{-10}$
1.5	100	101	-7.3	0.9	$5.2 \cdot 10^{-11}$
2.0	10	97	-7.4	1.0	$2.7 \cdot 10^{-10}$
2.0	100	101	-7.3	0.9	$9.6 \cdot 10^{-11}$

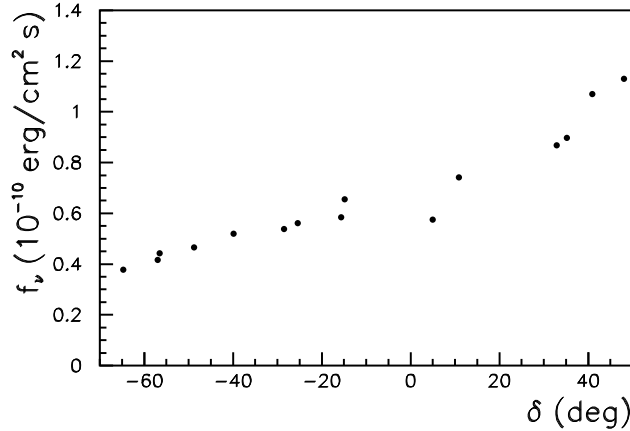


Fig. 2. NEMO-km³ sensitivity to neutrinos from microquasars versus source declination, for a livetime of 1 year. The worsening of the sensitivity with increasing declination is due to the decrease of the source visibility.

8 Conclusions

The possibility to detect TeV neutrinos from Galactic microquasars with the proposed NEMO-km³ underwater Čerenkov neutrino telescope has been investigated.

A Monte Carlo was carried out to simulate the expected neutrino-induced muon fluxes produced by point-like sources and by atmospheric neutrinos. The expected atmospheric muon background was also simulated. Muon tracks were propagated inside the detector using the ANTARES simulation tools, taking into account the water optical parameters measured in the Capo Passero site. Muon tracks were then reconstructed and the number of neutrino induced muons expected for microquasars was determined, according to differ-

ent theoretical neutrino flux predictions present in literature. These results were compared with the number of expected background events from atmospheric neutrinos and muons. We applied an event selection in order to reject the atmospheric background. The applied event selection is a combination of different criteria, chosen optimizing the detector sensitivity to neutrino fluxes coming from each microquasar. Eventually we calculated the expected number of events surviving the selection referring to 1 year of data taking.

Our results show that, assuming reasonable scenarios for TeV neutrino production, the proposed NEMO telescope could identify microquasars in a few years of data taking, with a discovery potential for at least few cases above the 5σ level, otherwise strongly constrain the neutrino production models and the source parameters.

Acknowledgments

We thank the ANTARES Collaboration for providing the detector simulation and track reconstruction codes, extensively used in this work. We thank also F.A. Aharonian, W. Bednarek and G.E. Romero for discussions and comments.

References

- [1] J. Learned, K. Mannaheim, *Ann. Rev. Part. Sci* 50 (2000) 679.
- [2] F. Halzen and D. Hopper, *Rep. Prog. Phys.* 65 (2002) 1025.
- [3] NEMO web page: <http://nemoweb.lns.infn.it>.
- [4] S. Chaty, *Proc. of Rencontres de Moriond, Very High Energy Phenomena in the Universe*, La Thuile, Italy, March 12-19, 2005 (astro-ph/0506008).
- [5] A. Levinson, E. Waxman, *Phys. Rev. Lett.* (2001) 87.171101.
- [6] C. Distefano, D. Guetta, E. Waxman, A. Levinson, *ApJ* 575 (2002) 378.
- [7] W. Bednarek, *ApJ* 631 (2005) 466.
- [8] F.A. Aharonian et al., *J. Phys. Conf. Ser.* 39 (2006) 408 (astro-ph/0508658).
- [9] F.A. Aharonian et al., *Science*, 309 (2005) 746.
- [10] H.R. Christiansen et al., *Phys.Rev.* D73 (2006) 063012.
- [11] G.E. Romero et al., *A&A* 410 (2003) L1.
- [12] G.E. Romero and M. Orellana, *A&A* 439 (2005) 237.

- [13] E. Migneco et al., Proc. of VLVnT2, Catania, Nov 8 - 11, 2005, NIM A, in press.
- [14] G. Riccobene et al., astro-ph/0603701, Astrop. Phys. (2006), submitted.
- [15] The NEMO Collaboration, *Study and characterization of a deep sea site for a km³ underwater neutrino telescope*, report to ApPEC (2002), available at <http://nemoweb.lns.infn.it/sitereport/>.
- [16] U.F. Katz, astro-ph/0606068, Proc. of VLVnT2, Catania, Nov 8 - 11, 2005, NIM A, in press; KM3NeT website: <http://www.km3net.org>.
- [17] J.A. Aguilar et al., astro-ph/0606229, Astropart. Phys. (2006), submitted; NIM A555 (2005) 132; ANTARES web page: <http://antares.in2p3.fr>.
- [18] Y. Becherini, ANTARES Collaboration, Proc. of VLVnT2, Catania, Nov 8 - 11, 2005, NIM A, in press.
- [19] D. Zaborov, ANTARES Collaboration, 2003, Proc. of VLVnT Workshop, Amsterdam, October 5-8 2003, <http://www.vlvnt.nl/proceeding>.
- [20] P. Sapienza, NEMO Collaboration, 2003, Proc. of VLVnT Workshop, Amsterdam, October 5-8 2003, <http://www.vlvnt.nl/proceeding>.
- [21] G. Ingelman, A. Edin, J. Rathsman, Comput. Phys. Commun. 101 (1997) 108.
- [22] P. Antonioli et al., Astropart. Phys. 7 (1997) 357.
- [23] R. Gandhi et al., Astropart. Phys. 5 (1996) 81.
- [24] A. Okada, Astrop. Phys. 2 (1994) 393.
- [25] A. Heijboer, 2004, *Track reconstruction and point source searches with Antares*, PhD dissertation, Universiteit van Amsterdam, Amsterdam, The Netherlands (<http://antares.in2p3.fr/>).
- [26] V. Agrawal et al., Phys. Rev. D53 (1996) 1314.
- [27] E.V. Bugaev et al., Phys. Rev. D58 (1998) 054001.
- [28] G.J. Feldman & R.D. Cousins, Phys. Rev. D 57 (1998) 3873.
- [29] R.A. Preston et al., ApJ 268 (1983) L23.
- [30] R.M. Hjellming & M.P. Rupen, Nature 375 (1995) 464.
- [31] L.F. Rodríguez & I.F. Mirabel, ApJ 511 (1999) 398.
- [32] C. Nipoti et al., MNRAS 361 (2005) 633.
- [33] M. Ackermann et al., IceCube Collaboration, Proc. of 29th ICRC gerackermann-M-abs1-og25-oral, Pune, India, (2005), <http://icrc2005.tifr.res.in/>.